

## Supporting Information

### Sterically-constrained tripodal phosphorus-bridged *tris*-pyridyl ligands

Schirin Hanf,<sup>a</sup> Raúl García-Rodríguez,<sup>a</sup> Andrew D. Bond,<sup>a</sup> Evamarie Hey-Hawkins<sup>b,\*</sup> and Dominic S. Wright<sup>a,\*</sup>

<sup>a</sup>. Chemistry Department, Cambridge University, Lensfield Road, CB2 1EW, Cambridge, UK.

<sup>b</sup>. Institute of Inorganic Chemistry, Faculty of Chemistry and Mineralogy, Leipzig University, Johannisallee 29, 04103 Leipzig, Germany.

## Representative NMR spectra for selected compounds

### NMR spectra of P(2-py)<sub>3</sub> (**1**)

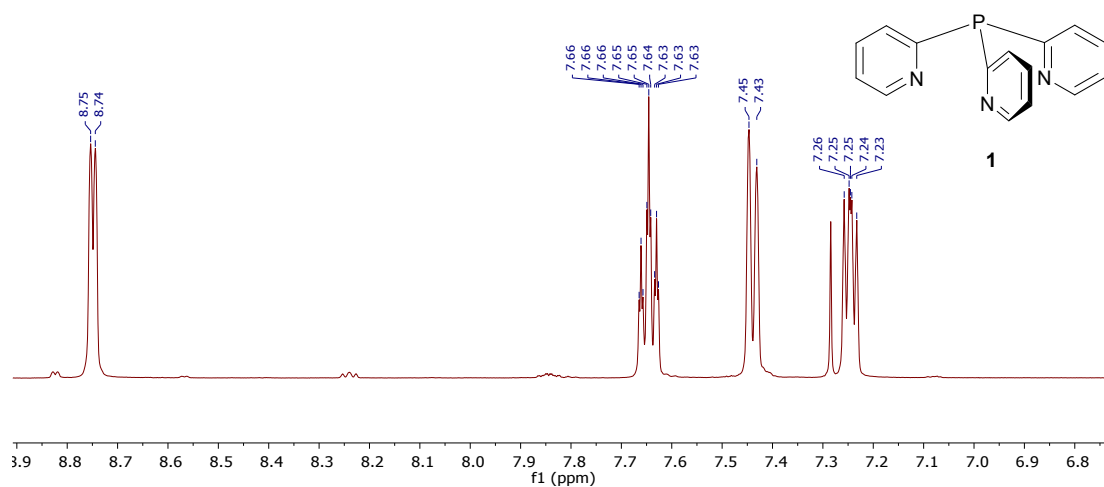


**Figure S1:** <sup>1</sup>H NMR (298 K, CDCl<sub>3</sub>, 500.20 MHz) spectrum of P(2-py)<sub>3</sub> (**1**).

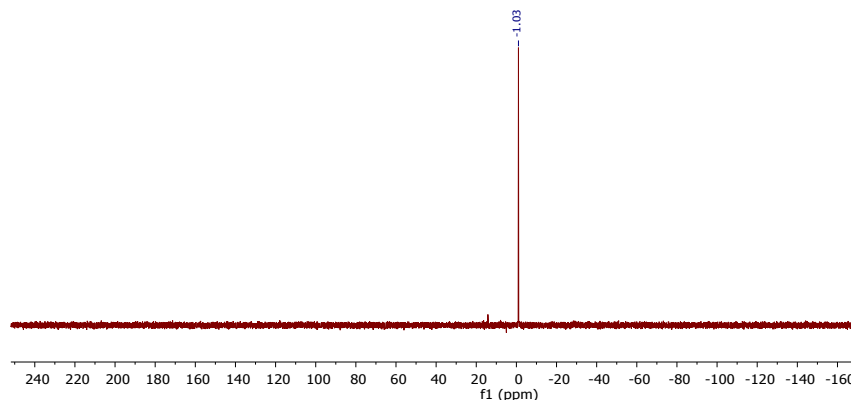


**Figure S2:** <sup>31</sup>P{<sup>1</sup>H} NMR (298 K, CDCl<sub>3</sub>, 202.48 MHz) spectrum of P(2-py)<sub>3</sub> (**1**).

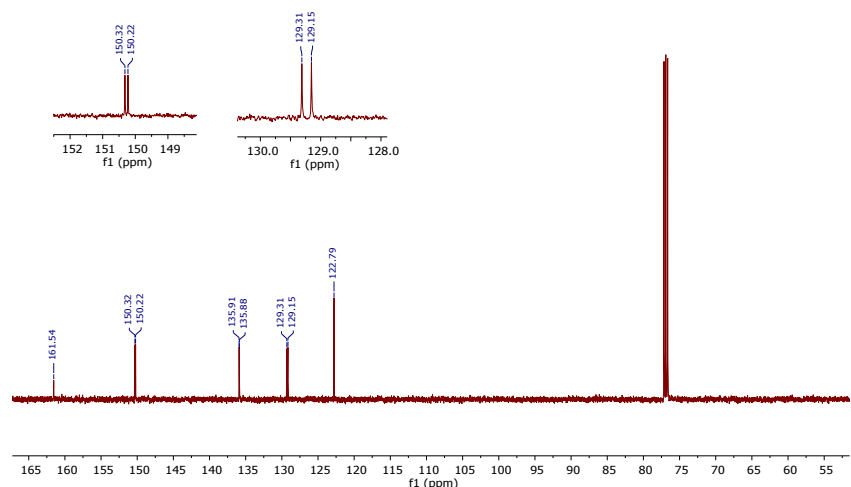


**Figure S3:** <sup>13</sup>C{<sup>1</sup>H} NMR (298 K, CDCl<sub>3</sub>, 125.78 MHz) spectrum of P(2-py)<sub>3</sub> (**1**).

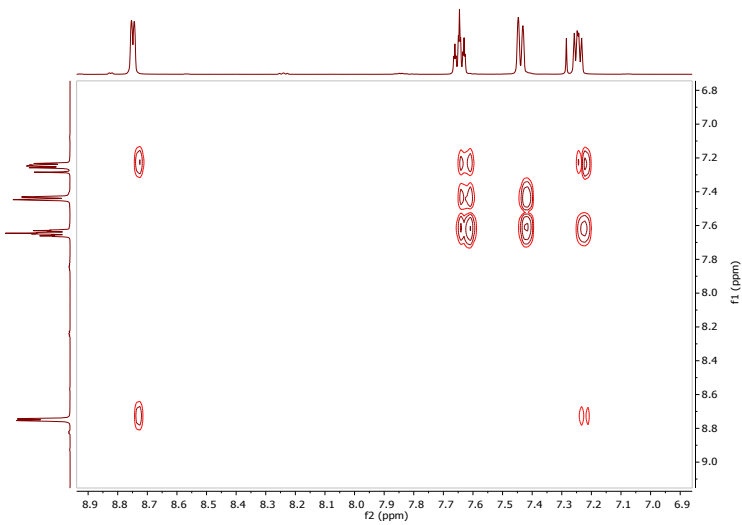


**Figure S4:**  $^1\text{H}$ - $^1\text{H}$  COSY (298 K,  $\text{CDCl}_3$ , 500.20 MHz) spectrum of  $\text{P}(\text{2-py})_3$  (**1**).

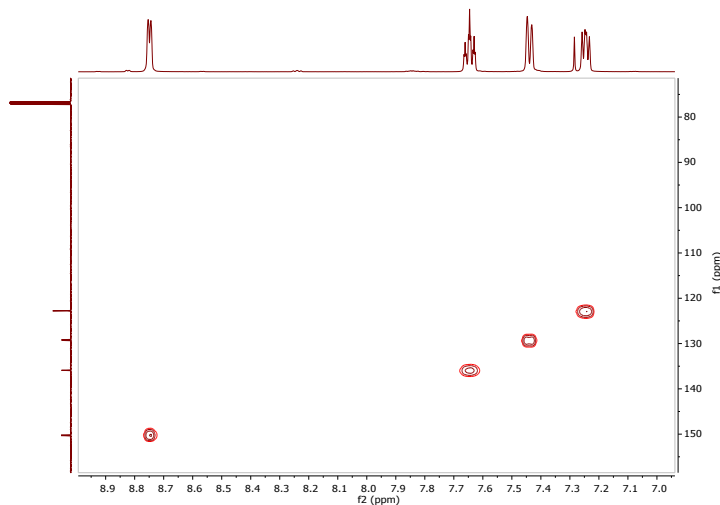


**Figure S5:**  $^1\text{H}$ - $^{13}\text{C}$  HMQC (298 K,  $\text{CDCl}_3$ , 500.20 MHz) spectrum of  $\text{P}(\text{2-py})_3$  (**1**).

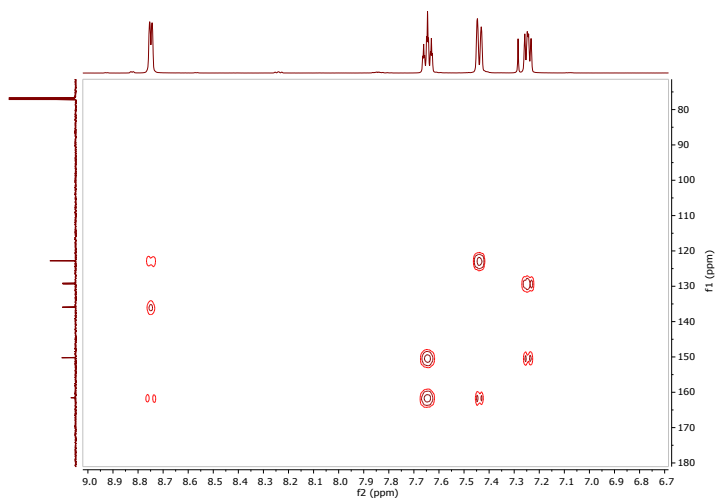


**Figure S6:**  $^1\text{H}$ - $^{13}\text{C}$  HMBC (298 K,  $\text{CDCl}_3$ , 500.20 MHz) spectrum of  $\text{P}(\text{2-py})_3$  (**1**).

NMR spectra of  $P(6\text{-Me-2-py})_3$  (**2**)

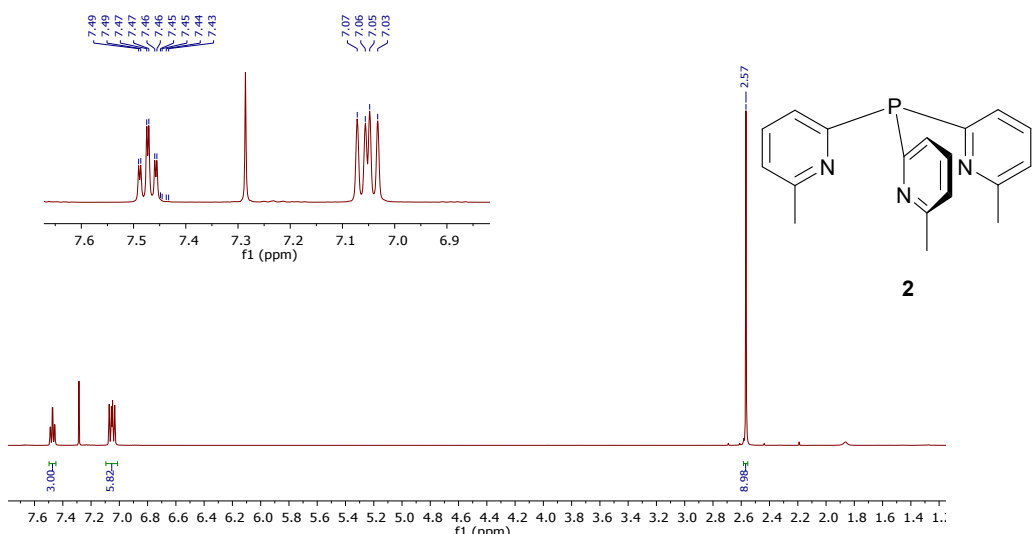


**Figure S7:**  $^1\text{H}$  NMR (298 K,  $\text{CDCl}_3$ , 500.20 MHz) spectrum of  $P(6\text{-Me-2-py})_3$  (**2**).

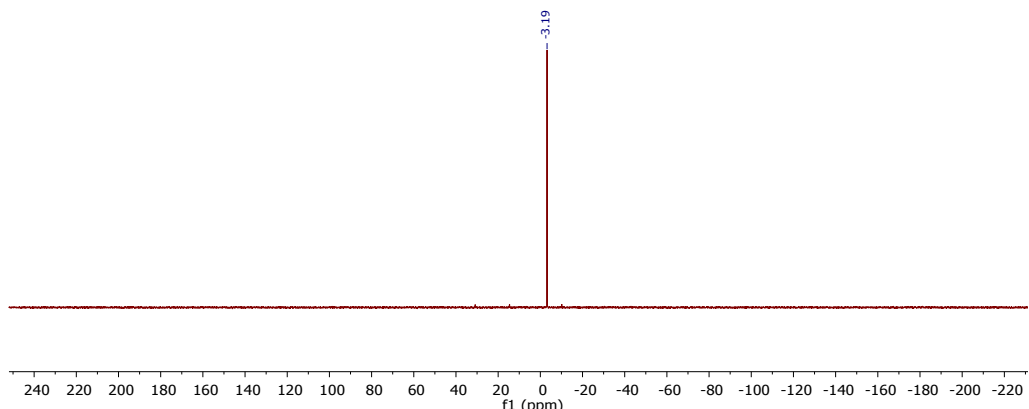


**Figure S8:**  $^{31}\text{P}\{\text{H}\}$  NMR (298 K,  $\text{CDCl}_3$ , 202.48 MHz) spectrum of  $P(6\text{-Me-2-py})_3$  (**2**).

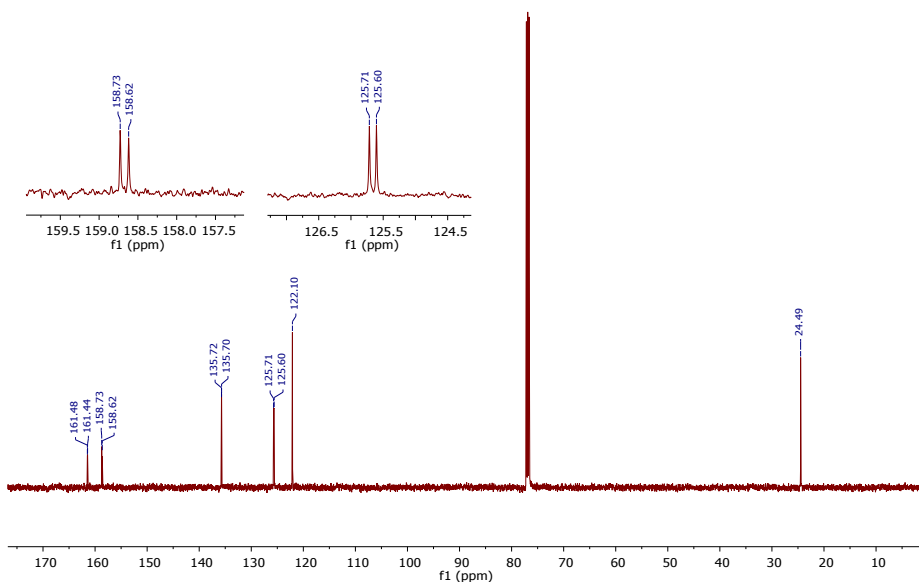


**Figure S9:**  $^{13}\text{C}\{\text{H}\}$  NMR (298 K,  $\text{CDCl}_3$ , 125.78 MHz) spectrum of  $P(6\text{-Me-2-py})_3$  (**2**).

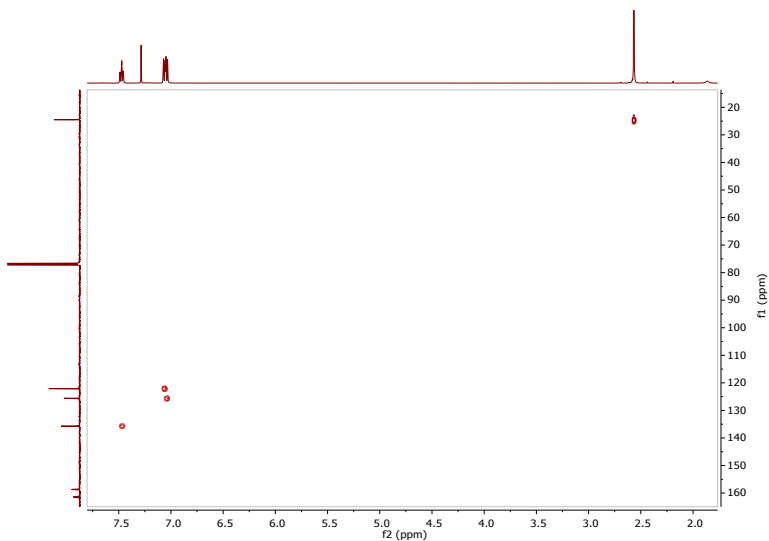


**Figure S10:**  $^1\text{H}$ - $^{13}\text{C}$  HMQC (298 K,  $\text{CDCl}_3$ , 500.20 MHz) spectrum of  $\text{P}(6\text{-Me-2-py})_3$  (**2**).

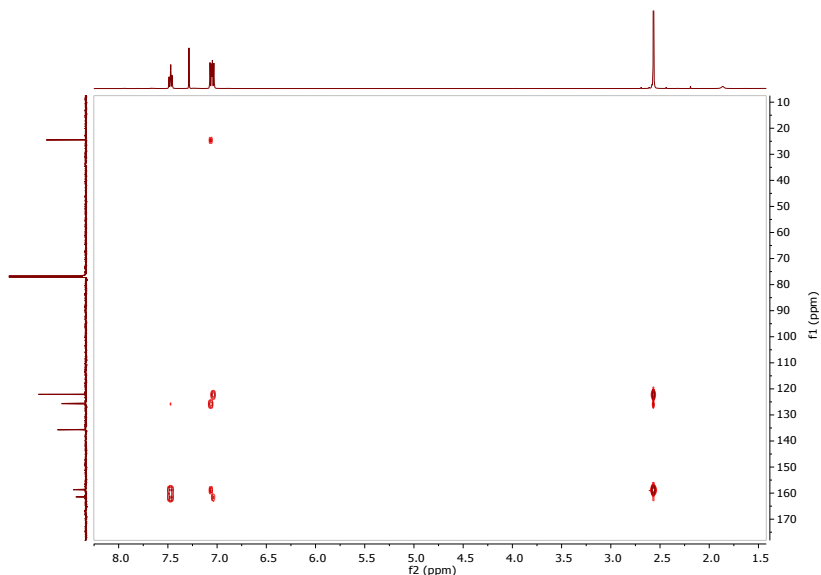


**Figure S11:**  $^1\text{H}$ - $^{13}\text{C}$  HMBC (298 K,  $\text{CDCl}_3$ , 500.20 MHz) spectrum of  $\text{P}(6\text{-Me-2-py})_3$  (**2**).

### NMR spectra of $\text{P}(6\text{-Br-2-py})_3$ (**3**)

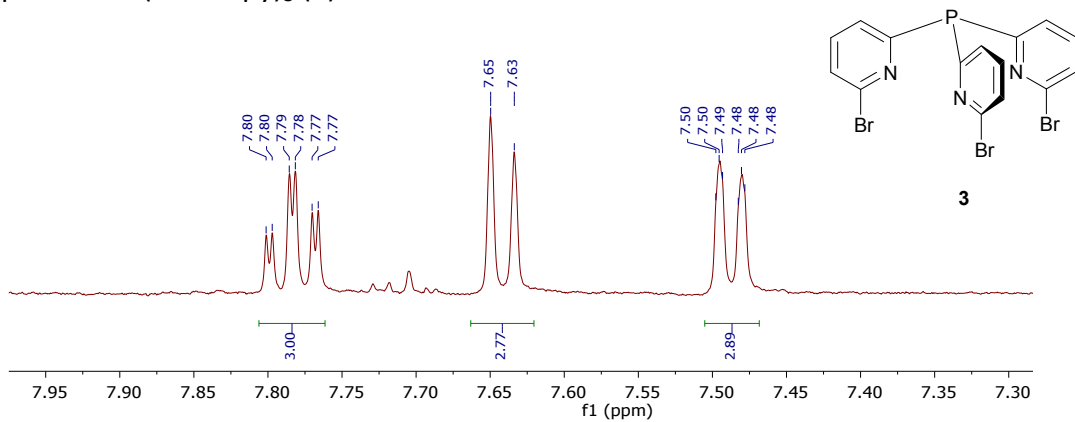


**Figure S12:**  $^1\text{H}$  NMR (298 K,  $\text{CD}_3\text{COCD}_3$ , 500.20 MHz) spectrum of  $\text{P}(6\text{-Br-2-py})_3$  (**3**).

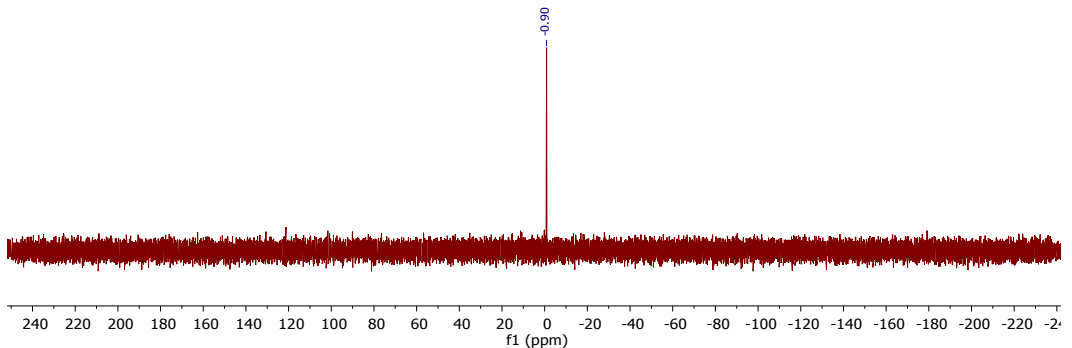


**Figure S13:**  $^{31}\text{P}\{\text{H}\}$  NMR (298 K,  $\text{CD}_3\text{COCD}_3$ , 202.48 MHz) spectrum of  $\text{P}(6\text{-Br-2-py})_3$  (**3**).

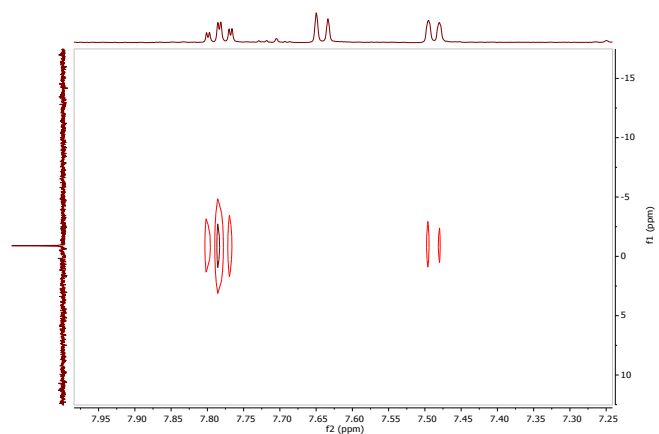


**Figure S14:**  $^1\text{H}$ - $^{31}\text{P}\{\text{H}\}$  HMQC (298 K,  $\text{CD}_3\text{COCD}_3$ , 500.20 MHz) spectrum of  $\text{P}(6\text{-Br-2-py})_3$  (**3**).

### NMR spectra of $[\{\text{P}(2\text{-py})_3\}_2\text{Fe}](\text{OTf})_2$ (**4**)

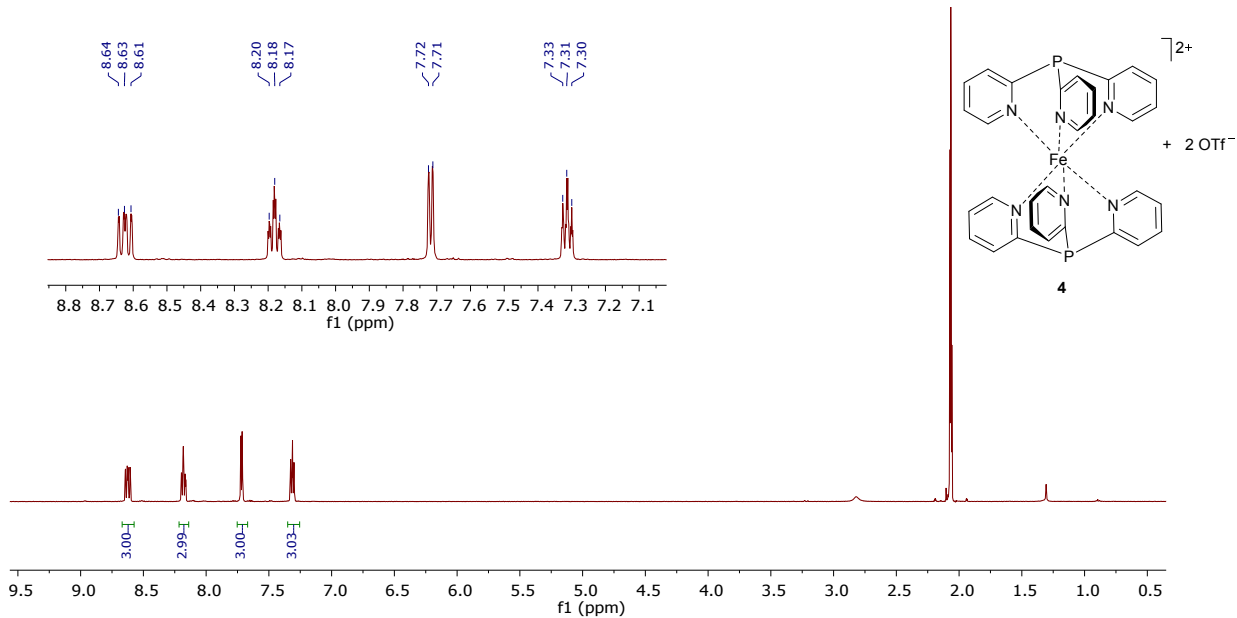


**Figure S15:**  $^1\text{H}$  NMR (298 K,  $\text{CD}_3\text{COCD}_3$ , 500.20 MHz) spectrum of  $[\{\text{P}(2\text{-py})_3\}_2\text{Fe}](\text{OTf})_2$  (**4**).

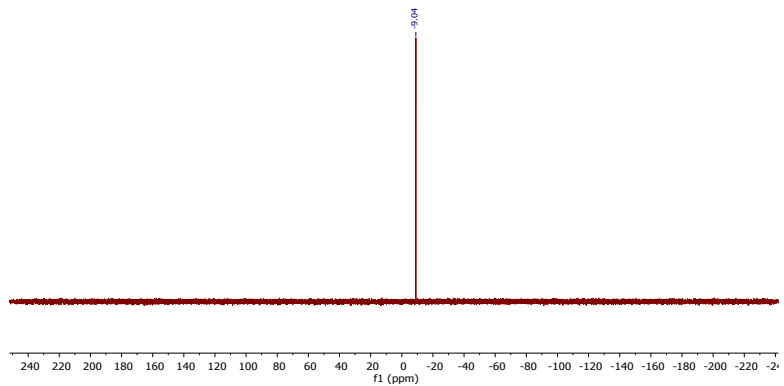


**Figure S16:**  $^{31}\text{P}\{\text{H}\}$  NMR (298 K,  $\text{CD}_3\text{COCD}_3$ , 202.48 MHz) spectrum of  $[{\{P(2\text{-py})_3\}}_2\text{Fe}](\text{OTf})_2$  (**4**).

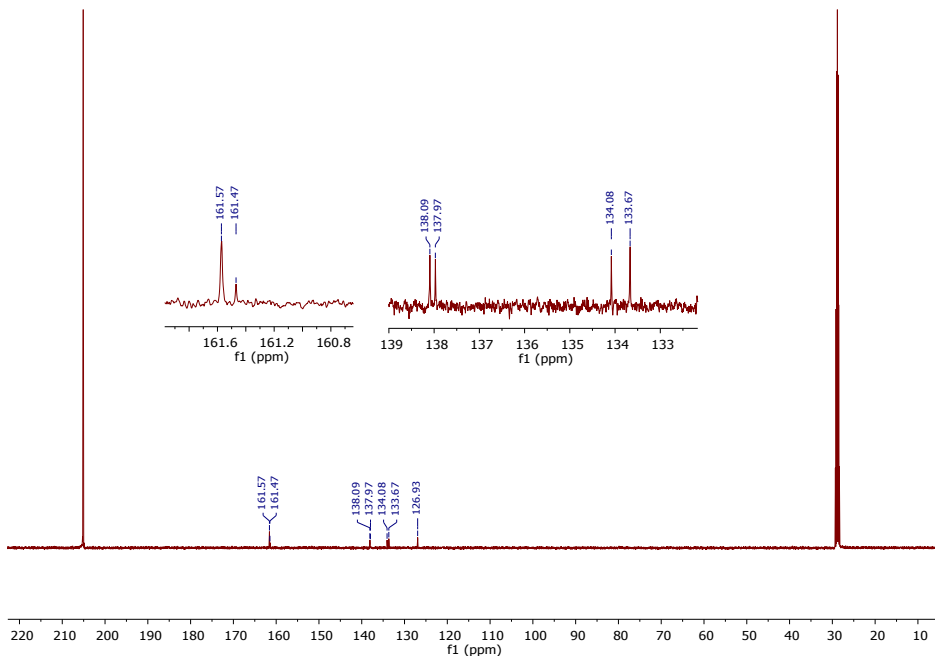


**Figure S17:**  $^{13}\text{C}\{\text{H}\}$  NMR (298 K,  $\text{CD}_3\text{COCD}_3$ , 125.78 MHz) spectrum of  $[{\{P(2\text{-py})_3\}}_2\text{Fe}](\text{OTf})_2$  (**4**).

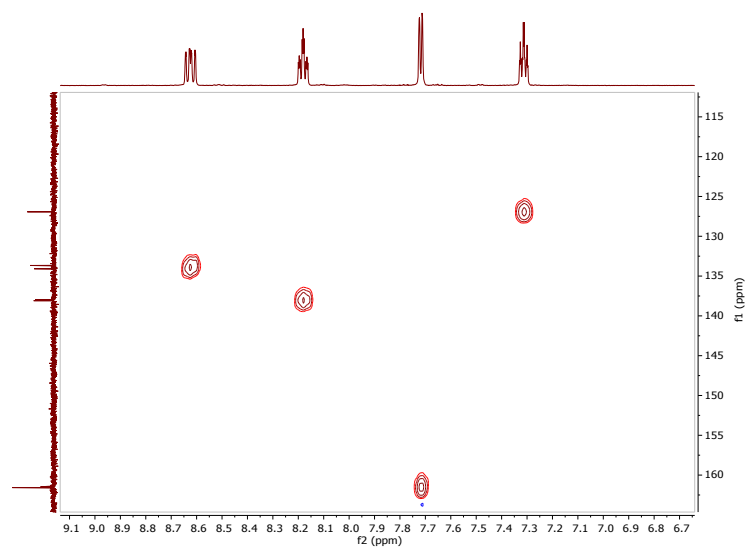


**Figure S18:**  $^1\text{H}$ - $^{13}\text{C}$  HMQC (298 K,  $\text{CD}_3\text{COCD}_3$ , 500.20 MHz) spectrum of  $[{\{P(2\text{-py})_3\}}_2\text{Fe}](\text{OTf})_2$  (**4**).

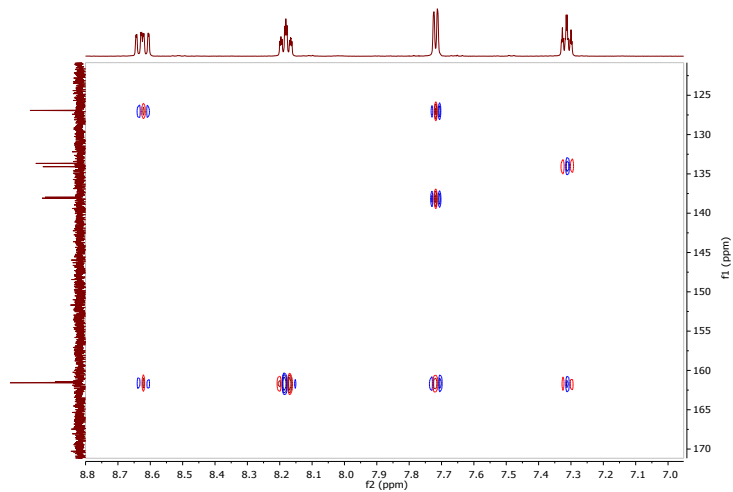


**Figure S19:**  $^1\text{H}$ - $^{13}\text{C}$  HMBC (298 K,  $\text{CD}_3\text{COCD}_3$ , 500.20 MHz) spectrum of  $[{\{P(2\text{-py})_3\}}_2\text{Fe}](\text{OTf})_2$  (**4**).

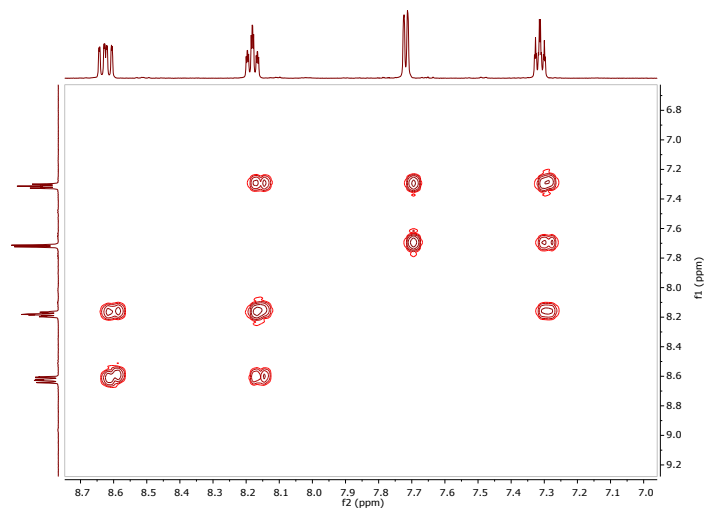


**Figure S20:**  $^1\text{H}$ - $^1\text{H}$  COSY (298 K,  $\text{CD}_3\text{COCD}_3$ , 500.20 MHz) spectrum of  $[{\{P(2\text{-py})_3\}}_2\text{Fe}](\text{OTf})_2$  (**4**).

### NMR spectra of $[(\text{MeCN})_3\text{Cu}\{P(6\text{-Me-2-py})_3\}\text{Cu}(\text{MeCN})](\text{PF}_6)_2$ (**7**)

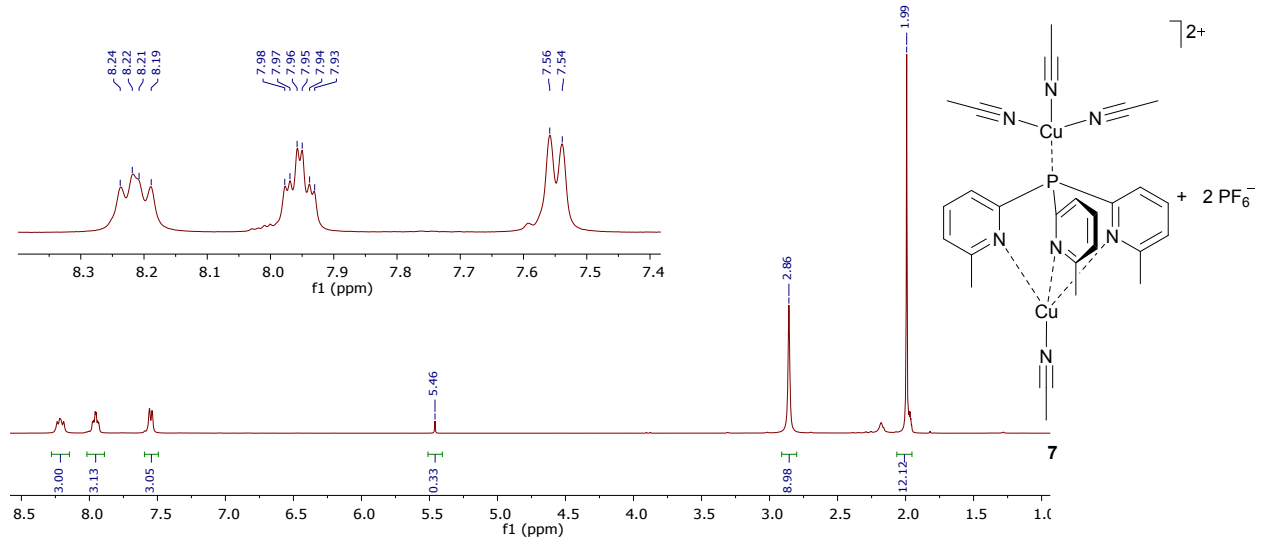


**Figure S21:**  $^1\text{H}$  NMR (298 K,  $\text{CD}_3\text{CN}$ , 400.13 MHz) spectrum of  $[(\text{MeCN})_3\text{Cu}\{P(6\text{-Me-2-py})_3\}\text{Cu}(\text{MeCN})](\text{PF}_6)_2$  (**7**).

Note: The acetonitrile solvent residual signal overlaps with the signal of the coordinated  $\text{CH}_3\text{CN}$  molecules at 1.99 ppm. Furthermore, the peak at 5.46 ppm arises from  $\text{CH}_2\text{Cl}_2$ .

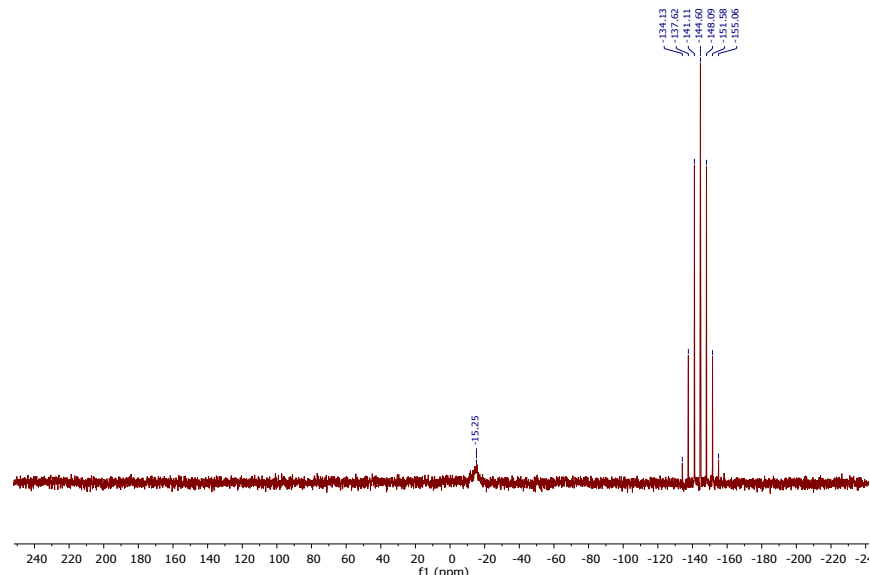


**Figure S22:**  $^{31}\text{P}\{\text{H}\}$  NMR (298 K,  $\text{CD}_3\text{CN}$ , 202.48 MHz) spectrum of  $[(\text{MeCN})_3\text{Cu}\{\text{P}(6\text{-Me-2-py})_3\}\text{Cu}(\text{MeCN})](\text{PF}_6)_2$  (**7**).

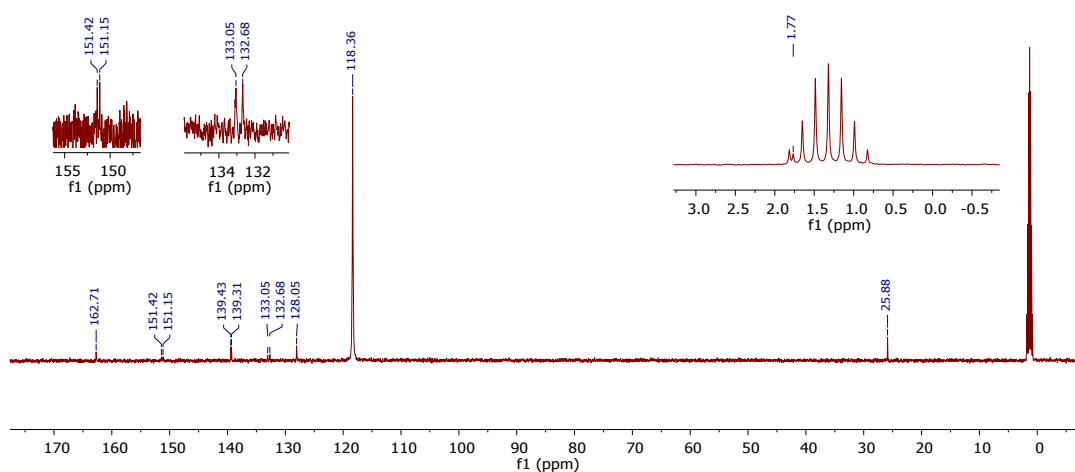


**Figure S23:**  $^{13}\text{C}\{\text{H}\}$  NMR (298 K,  $\text{CD}_3\text{CN}$ , 125.78 MHz) spectrum of  $[(\text{MeCN})_3\text{Cu}\{\text{P}(6\text{-Me-2-py})_3\}\text{Cu}(\text{MeCN})](\text{PF}_6)_2$  (**7**).

Note: The solvent residual peak of acetonitrile (septet at 1.32 ppm) overlaps with the signal of the coordinated  $\text{CH}_3\text{CN}$  molecules (1.77 ppm). The same observation was made for the second solvent residual peak of acetonitrile, which also overlaps with the signal of the coordinated  $\text{CH}_3\text{CN}$  molecules at 118.36 ppm.

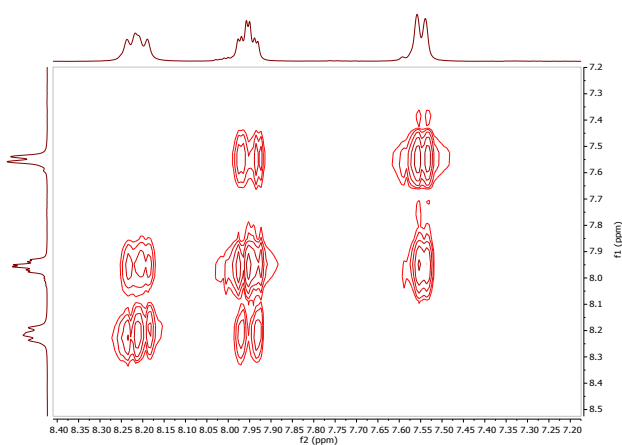


**Figure S24:**  $^1\text{H}$ - $^1\text{H}$  COSY (298 K,  $\text{CD}_3\text{CN}$ , 400.13 MHz) spectrum of  $[(\text{MeCN})_3\text{Cu}\{\text{P}(6\text{-Me-2-py})_3\}\text{Cu}(\text{MeCN})](\text{PF}_6)_2$  (**7**).

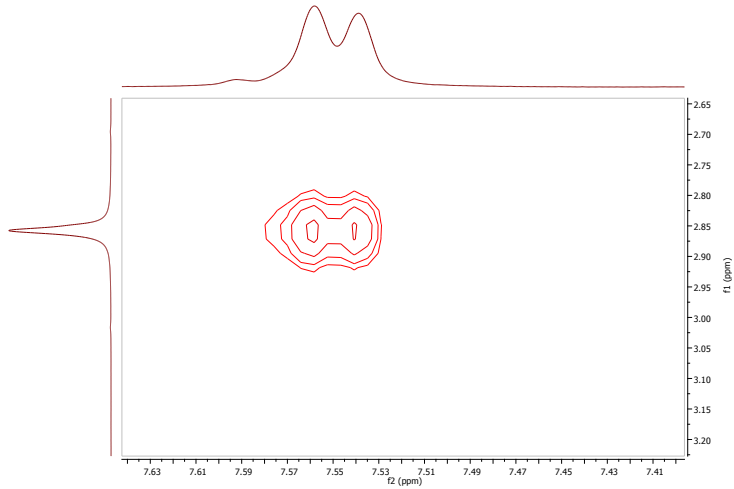


**Figure S25:** Section of the  $^1\text{H}$ - $^1\text{H}$  NOESY (298 K,  $\text{CD}_3\text{CN}$ , 400.13 MHz) spectrum of  $[(\text{MeCN})_3\text{CuP(6-Me-2-py)}_3\text{Cu}(\text{MeCN})](\text{PF}_6)_2$  (**7**).

Note: The crosspeak between H(5) and the  $\text{CH}_3$  group of the  $\text{P(6-Me-2-py)}_3$  ligand (**2**) in the  $^1\text{H}$ - $^1\text{H}$  NOESY spectrum of **7** arises from intramolecular cross-relaxation of protons, which are in close spatial proximity. The observation of this crosspeak confirms the assignment of H(5). This was the only crosspeak observed between a pyridyl-H and the 6- $\text{CH}_3$ -group.

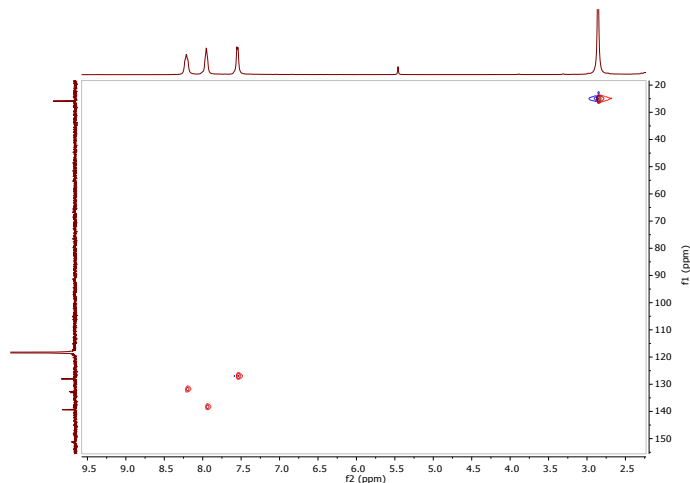


**Figure S26:**  $^1\text{H}$ - $^{13}\text{C}$  HMQC (298 K,  $\text{CD}_3\text{CN}$ , 500.20 MHz) spectrum of  $[(\text{MeCN})_3\text{CuP(6-Me-2-py)}_3\text{Cu}(\text{MeCN})](\text{PF}_6)$  (**7**).

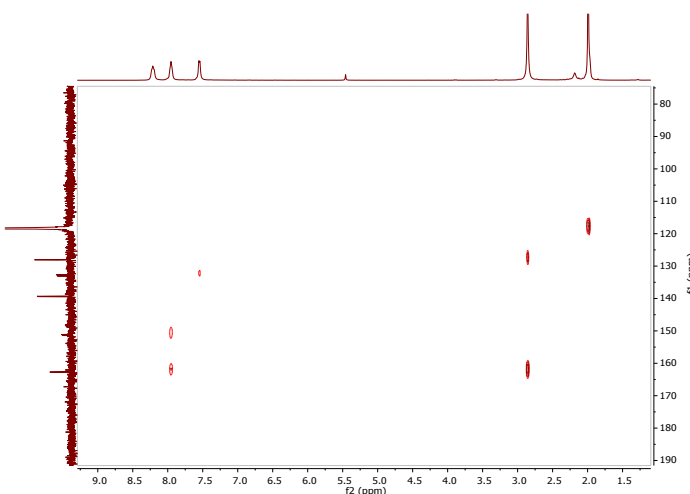


**Figure S27:**  $^1\text{H}$ - $^{13}\text{C}$  HMBC (298 K,  $\text{CD}_3\text{CN}$ , 500.20 MHz) spectrum of  $[(\text{MeCN})_3\text{CuP(6-Me-2-py)}_3\text{Cu}(\text{MeCN})](\text{PF}_6)$  (**7**).

## UV-visible spectroscopy

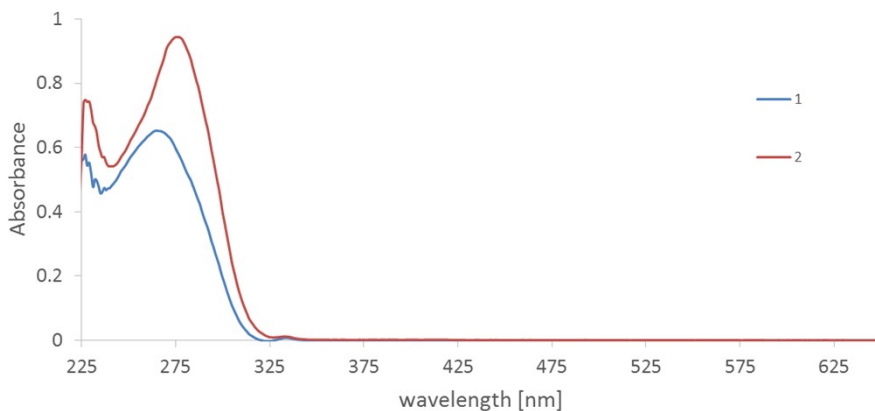


**Figure S28:** UV-visible spectra of the ligands **1** (blue) and **2** (red). Spectra were recorded in  $\text{CH}_2\text{Cl}_2$  (both at a concentration of  $5.0 \cdot 10^{-5} \text{ mol L}^{-1}$ ). Background solvent corrections were applied.

**Table S1:** Molar extinction coefficients calculated from UV-visible spectra (all at a concentration of  $5.0 \cdot 10^{-5} \text{ mol L}^{-1}$ )

Compound	Solvent	Wavelength $\lambda$ [nm]	Absorbance	Molar extinction coefficient $\epsilon \left[ \frac{\text{L}}{\text{cm} \cdot \text{mol}} \right]$
<b>1</b>	$\text{CH}_2\text{Cl}_2$	268.0	0.649	12976.5
<b>2</b>	$\text{CH}_2\text{Cl}_2$	281.0	0.905	18107.2
<b>4</b>	$\text{CH}_2\text{Cl}_2$	475.0	0.592	11834.3
		379.9	0.411	8227.6
		300.9	0.155	3091.5
		267.0	1.850	37003.1
<b>4</b>	MeOH	476.0	0.491	9816.5
		382.0	0.338	6751.2
		297.0	0.179	3579.5
		267.0	1.598	31915.5
<b>5-toluene</b>	$\text{CH}_3\text{CN}$	367.1	0.455	9102.5
		313.9	0.784	15682.3
		276.0	1.519	30379.6
<b>6-2THF</b>	MeOH	276.9	0.434	8685.3
<b>7</b>	$\text{CH}_3\text{CN}$	363.0	0.202	4036.6
		276.9	1.517	30344.8

## Single-crystal X-ray crystallography

**Table S2:** Crystallographic parameters.

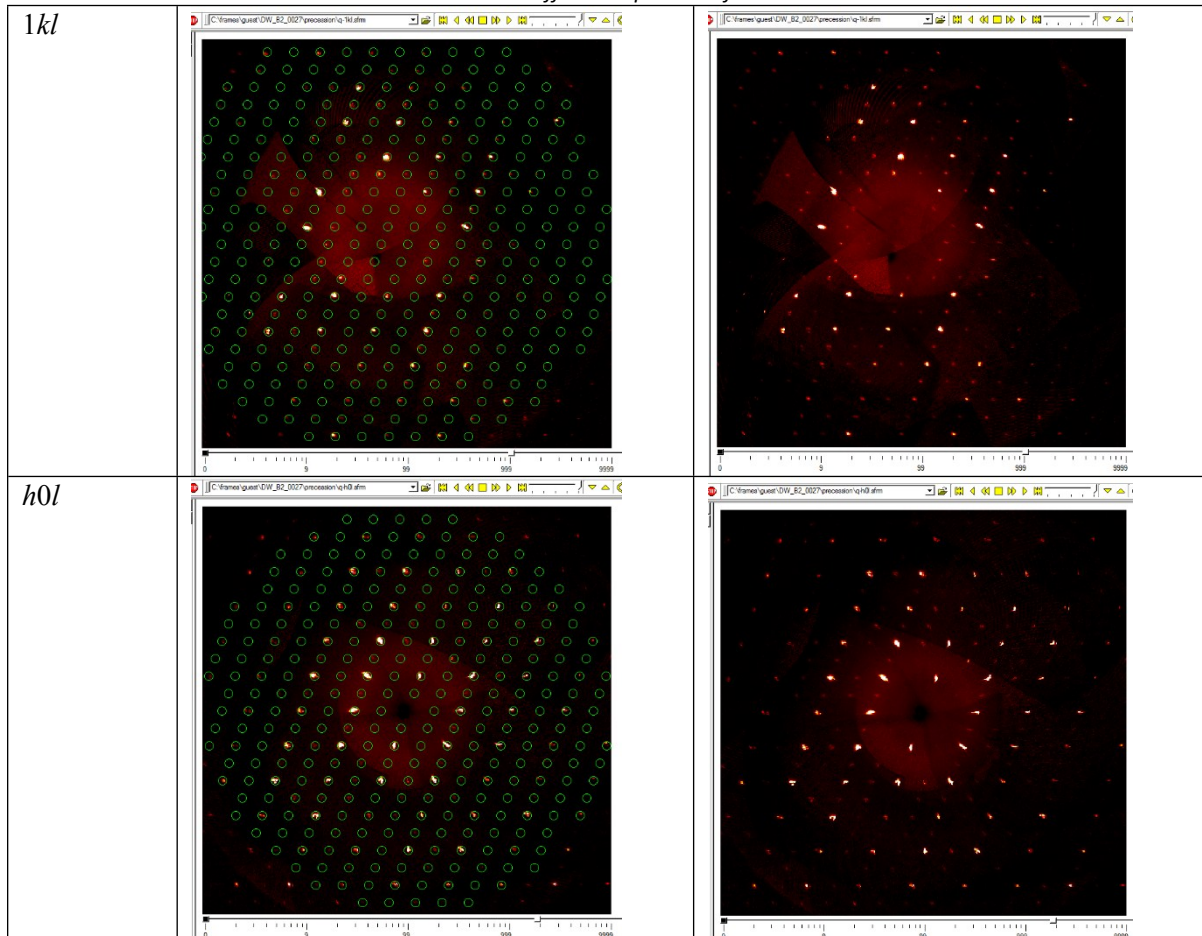
Compound reference	<b>2</b>	<b>3</b>	<b>4</b>	<b>5.toluene</b>	<b>6.2THF</b>	<b>7</b>
Chemical formula	$\text{C}_{18}\text{H}_{18}\text{N}_3\text{P}$	$\text{C}_{15}\text{H}_9\text{Br}_3\text{N}_3\text{P}$	$\text{C}_{30}\text{H}_{24}\text{FeN}_6\text{P}_2^{2+}$ $(\text{CF}_3\text{O}_3\text{S}^-)_2$	$\text{C}_{18}\text{H}_{18}\text{Cl}_2\text{FeN}_3\text{P} \cdot$ $\text{C}_7\text{H}_8$	$\text{C}_{19}\text{H}_{18}\text{ClF}_3\text{FeN}_3\text{O}$ $\cdot \text{PS} \cdot \text{C}_4\text{H}_8\text{O}$	$\text{C}_{26}\text{H}_{30}\text{Cu}_2\text{N}_7\text{P}$ $^{2+}(\text{PF}_6^-)_2$
Formula mass	307.32	501.95	884.48	526.21	619.80	888.56
Crystal system	trigonal	trigonal	monoclinic	triclinic	monoclinic	triclinic
$a/\text{\AA}$	30.7488(8)	15.7876(6)	17.6327(9)	8.0155(3)	13.7879(4)	8.2686(5)
$b/\text{\AA}$	30.7488(8)	15.7876(6)	20.0111(11)	10.7101(4)	8.6473(2)	14.9441(9)
$c/\text{\AA}$	11.8199(4)	11.1637(5)	19.8093(10)	15.0458(6)	22.5638(6)	14.9496(8)
$\alpha/^\circ$	90	90	90	98.595(2)	90	78.976(2)
$\beta/^\circ$	90	90	91.836(2)	99.108(2)	95.0326(12)	80.942(2)
$\gamma/^\circ$	120	120	90	91.742(2)	90	84.159(2)
Unit cell volume/ $\text{\AA}^3$	9678.3(6)	2409.7(2)	6986.1(6)	1259.09(8)	2679.87(12)	1785.67(18)
Temperature/K	180(2)	180(2)	180(2)	180(2)	180(2)	180(2)
Space group	$R\bar{3}c$	$R\bar{3}c$	$P2_1/n$	$P\bar{1}$	$P2/c$	$P\bar{1}$

Z	24	6	8	2	4	2
Radiation type	CuK $\alpha$					
Absorption coefficient, $\mu/\text{mm}^{-1}$	1.495	10.247	6.234	7.489	7.225	3.598
No. of reflections measured	35814	7384	103989	14375	32629	45856
No. of independent reflections	3769	941	12364	4367	4745	6267
$R_{\text{int}}$	0.036	0.062	0.054	0.042	0.036	0.031
Final R1 values ( $I > 2\sigma(I)$ )	0.028	0.033	0.039	0.045	0.036	0.049
Final wR( $F^2$ ) values ( $I > 2\sigma(I)$ )	0.072	0.061	0.094	0.092	0.088	0.126
Final R1 values (all data)	0.031	0.039	0.052	0.059	0.042	0.054
Final wR( $F^2$ ) values (all data)	0.074	0.062	0.102	0.098	0.094	0.130
Goodness of fit on $F^2$	1.05	1.09	1.02	1.06	1.07	1.03
Flack x determined using quotients $[(I+)-(I-)]/[(I+)+(I-)]$	0.03(1)	-0.01(3)				

#### Note regarding the structures of **2** and **3**

The structures of **2** (methyl derivative) and **3** (bromo derivative) are very closely comparable. However, **2** appears to adopt a superstructure with a unit-cell volume four times that of **3**. While **3** contains only  $\frac{1}{4}$  of a molecule in the asymmetric unit, **2** contains  $1+\frac{1}{4}$ . The structure of **2** contains local translations that amount to  $C$ -centring ( $\frac{1}{4}, \frac{1}{2}, 0$ ) in the reported *R*-centred cell. If these translations are considered to be real, the structure can be described with a subcell essentially identical to **3**. However, reconstructed precession images show clearly that the additional diffraction peaks are present and that the supercell is appropriate (Figure S29). For **3**, there is no sign of any additional diffraction peaks to indicate a larger cell. Thus, we conclude that the supercell structure for **2** is genuine, at least for the crystal examined. Refining **2** in the smaller cell analogous to **3** does produce a satisfactory refinement, but with somewhat elongated displacement ellipsoids, especially for the methyl group (of which there is only one unique in that representation) (Figure S30).

**Figure S29:** Reconstructed precession images for **2**, showing the consistency between the diffraction pattern and the reported supercell description indicated by the predicted reflection positions (green circles). No such additional spots appear in the diffraction pattern of **3**.



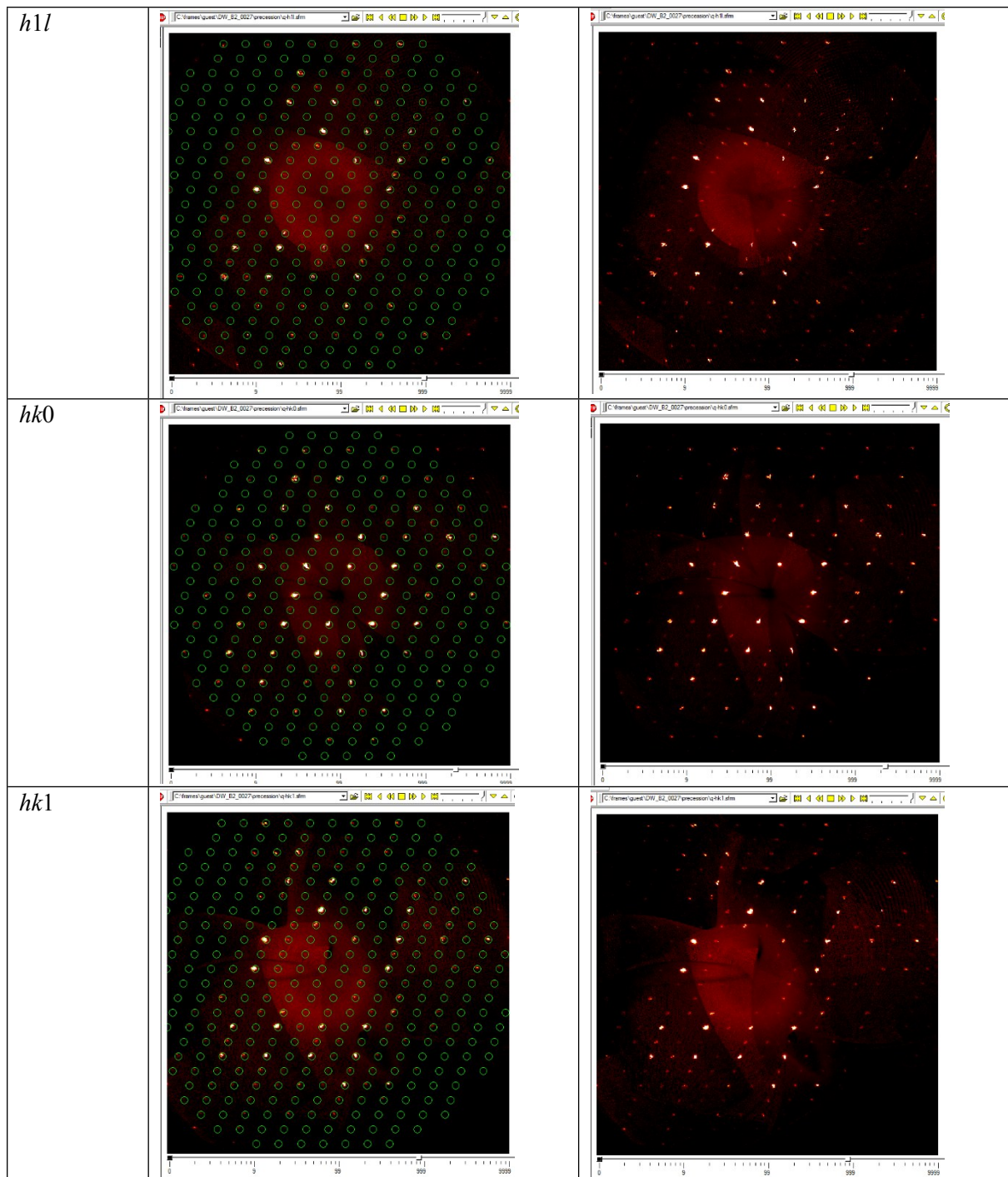


**Figure S30.** Displacement ellipsoid plot for the asymmetric unit of **2** in the subcell analogous to **3**.

